

Dark Current Compensation of a CMOS Image Sensor by Using In-Pixel Temperature Sensors

Accel Abarca^{1,2}, Albert Theuwissen^{1,3}

¹Delft University of Technology, Electronic Instrumentation Lab., Mekelweg 4, 2628CD, Delft, The Netherlands.

²now with INL – International Iberian Nanotechnology Lab., Avenida Mestre José Veiga s/n, 4715-330, Braga, Portugal; accel.abarca@inl.int

³Harvest Imaging, Witte Torenwal 8E, app. 2.1, 3960 Bree, Belgium; albert@harvestimaging.com

Abstract—In this paper a novel technique to compensate for dark current of a CMOS image sensor (CIS) by using in-pixel temperature sensors (IPTs) is presented. The IPTs are integrated in the same layer as the image pixels and use the same readout circuit as the pixels. Therefore, the real temperature variations in the pixel array can be measured as well as the thermal distribution across the array. The dark current compensation can be carried out locally by creating a dark reference frame from the in-pixel temperature measurements and the temperature behavior of the dark current. The artificial dark reference frame is subtracted from the actual images to reduce/cancel the dark signal level of the generated images.

Keywords—CIS, in-pixel temperature sensors, dark current compensation

I. INTRODUCTION

Over the last few decades the growing market for portable devices has pushed the CMOS active pixel sensor (APS) industry to rapidly improve CMOS technology performance. The wide use of the APS is related to its high integrability, low cost, and low power consumption [1], [2]. CMOS APS image sensors are widely used in a variety of applications, ranging from medical to military. The dark current is one of the key parameters which characterizes the performance of the APS, where a low dark current is preferred. However, the continuous downscaling of CMOS technology to sub-micron sizes while keeping dark current levels low is a challenge [3], [4]. The dark current is one of the major components of fixed pattern noise (FPN) in CIS as well as an important contributor to temporal random noise [5]. Large dark current in a CIS leads to high noise, non-uniformity, and a reduced dynamic range [6]. The dark current exhibits a linear behavior over exposure time, and an exponential behavior over temperature. In fact, the dark current doubles every $\sim 5\text{-}10$ °C [7], [8], [9]. A conventional technique for dark current compensation is to take a dark reference frame during the picture acquisition at a certain exposure time with closed mechanical shutter, and subtract this dark frame from the images. However, the temperature must be kept constant during the acquisition to avoid any dark current variation. Also, some cameras (such as mobile phones) do not have a shutter, therefore obtaining the dark reference frame is not possible. A technique to compensate for dark current has been proposed by [10]. In [10] the compensation involves using a Miller differential amplifier with the non-inverting input connected to a dummy shielded photodiode and the inverting input connected

to an active photodiode. The offset (dark current level) provided by the dummy shielded photodiode is sampled and subtracted from the video signal (including the dark current from the active photodiode) compensating for the dark current of the active pixel. However, the mismatch between the active photodiode and the dummy shielded photodiode is not addressed in [10]. Another technique has been proposed by [11], where the dark current of hundreds of hot pixels is used as a temperature indicator across the pixel array. The dark current of the hot pixels has been calibrated in a temperature range of -40 °C and 8 °C, and it is used to predict the dark current level of the rest of the pixels. However, the compensation is limited to the temperature range of -40 °C and 8 °C and no information about the accuracy of the hot pixels acting as temperature sensors is provided.

We propose using the absolute temperature information provided by the in-pixel temperature sensors (IPTs) to create a dark reference frame at a particular exposure time to compensate for dark current across the pixel array without the need of a mechanical shutter and without the request for constant temperature. The in-pixel temperature sensors have been proposed in our previous works, where the use of parasitic substrate bipolar temperature sensor pixel (Tixel) [12], and the use of the imaging pixel itself as a temperature sensor [13], [14] have been shown and proved. In this paper, the CIS and the IPTs are characterized in a temperature range of -40 °C and 90 °C. The dark current exhibits the typical exponential behaviour, increasing with the temperature, while the IPTs show good accuracy in the above-mentioned temperature range. The dark current can be compensated by 82% of its median value and the non-uniformity is reduced by 63% when using the IPTs, which proves the quality of the generated artificial dark frame.

II. DARK CURRENT COMPENSATION

A. CMOS Image Sensor

The test CIS is composed of a 60×70 pixel array, row and column decoders, a programmable gain amplifier (PGA), a sample and hold circuit (S/H), an output buffer, and an external 16 bits ADC, as shown in Figure 1. The IPT is based on the nMOS source follower (nSFTS) of the 4T pixel itself. Thus, the 4T pixel can be used either as a pixel or as a temperature sensor.

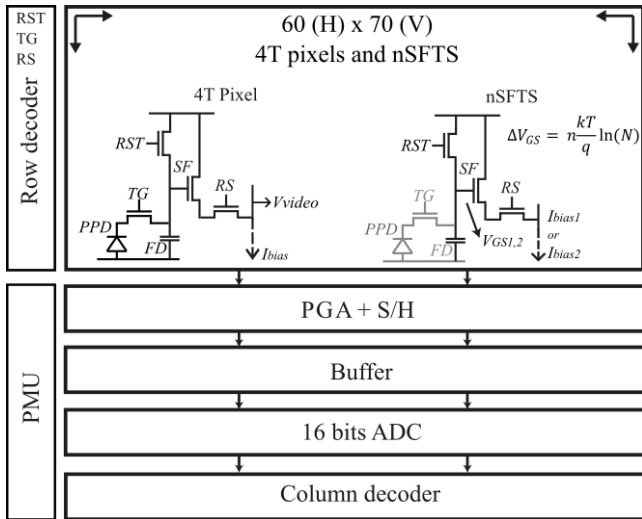


Figure 1: Block diagram of the CIS.

When the nSFTS is biased by sequential ratiometric currents in a ratio N ($N = I_{bias2}/I_{bias1}$), then the differential gate-source voltage (ΔV_{GS}) is proportional to the absolute temperature (PTAT), as shown in (1) (the TG of the pixel must be switched off):

$$\Delta V_{GS} = n \frac{kT}{q} \ln(N) \rightarrow T = \frac{q \Delta V_{GS}}{nkT \ln(N)} \quad (1)$$

where n is a process parameter, k is the Boltzmann constant, T is the absolute temperature, and q is the single electro-charge. As the pixel's readout offers the opportunity to use correlated double sampling (CDS) performed by the PGA and S/H, it becomes natural to use the same readout system for the nSFTSs in order to obtain the differential gate-source voltage.

The sensor was designed and fabricated in a standard CIS 0.18 μm TowerJazz technology.

B. Dark Current Compensation Technique

The CMOS imager pixel can be used as a standard pixel or as a temperature sensor, but not simultaneously. Nevertheless, it is possible to take a temperature frame (TF) in between the video frames, as shown in Figure 2.

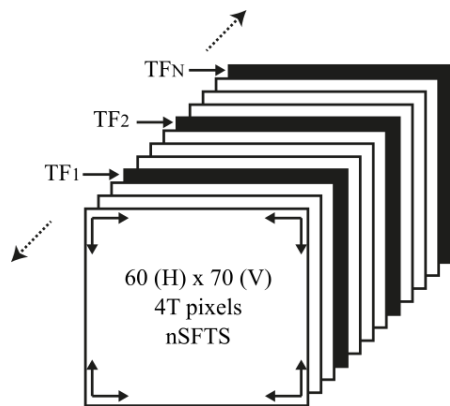


Figure 2: Temperature frames that are taken in between image frames.

As the dark current depends on temperature, it can be compensated by using the knowledge of the absolute temperature and thermal distribution provided by the TF. Thus, the dark current compensation is done locally at pixel level. It is well known that the dark current exhibits an exponential behavior over temperature, as shown in equation (2).

$$I_{dark} = A \cdot e^{B \cdot T} \quad (2)$$

Where A and B are constants defined during measurements.

Then, the nSFTSs provide absolute temperature based on ΔV_{GS} across the pixel array in the form of (3):

$$\Delta V_{GS} = C \cdot T + D \quad (3)$$

where C and D are constants.

Combining equations (2) and (3), the temperature value is replaced in the exponential fit and the absolute dark current level is obtained.

$$I_{dark} = A \cdot e^{F \cdot \Delta V_{GS}} \quad (4)$$

Where constant F combines B , C , and D .

As the dark signal (S_{dark}) linearly depends on the exposure time (t_{exp}), the absolute dark signal can be calculated from the dark current value at a certain exposure time.

$$\begin{aligned} S_{dark} &= I_{dark} \cdot t_{exp} \\ S_{dark} &= A \cdot e^{F \cdot \Delta V_{GS}} \cdot t_{exp} \end{aligned} \quad (5)$$

Thus, by applying this algorithm to each pixel across the pixel array, an artificial dark frame can be generated from the absolute temperature information provided by the nSFTSs without the need of a mechanical shutter and the request for constant temperature. Constants (A , B , C , D , and F) are obtained from measurements.

III. MEASUREMENT RESULTS AND DISCUSSION

The measurement setup consists of a PCB, FPGA, a PC with Quartus and LabView, and a temperature-controlled oven. The test chip is mounted on the PCB that provides all the power supplied to the chip and contains the 16-bit ADC. The FPGA generates all the control signals for the chip and for the ADC. The FPGA is configured by using Quartus, and the data of the chip is collected by utilizing LabView. Measurements have been performed over a temperature range of -40 $^{\circ}\text{C}$ and 90 $^{\circ}\text{C}$. As a temperature reference, a calibrated Pt-100 thermistor was used. After averaging 100 frames and all pixels, the average dark current exhibits two types of temperature behavior depending on the temperature range, as shown in Figure 3. At low temperatures, the average dark current increases 1.08 times every 5 $^{\circ}\text{C}$ and it is mainly due to depletion I_{dark} . While at high temperatures it increases 1.8 times every 5 $^{\circ}\text{C}$, and diffusion I_{dark} dominates. Therefore, the dark current becomes more relevant at temperatures above 35 $^{\circ}\text{C}$. The dark current for temperatures above 35 $^{\circ}\text{C}$ is shown in Figure 4.

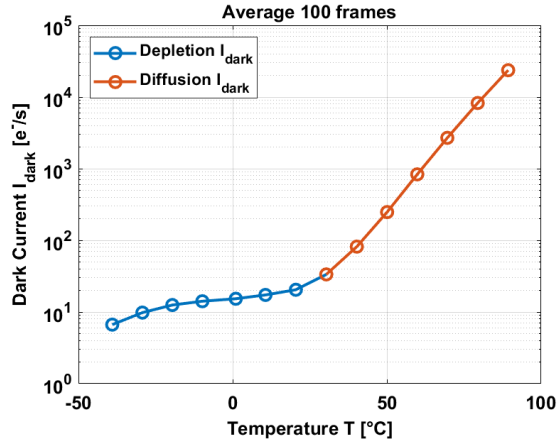


Figure 3: Dark current over temperature.

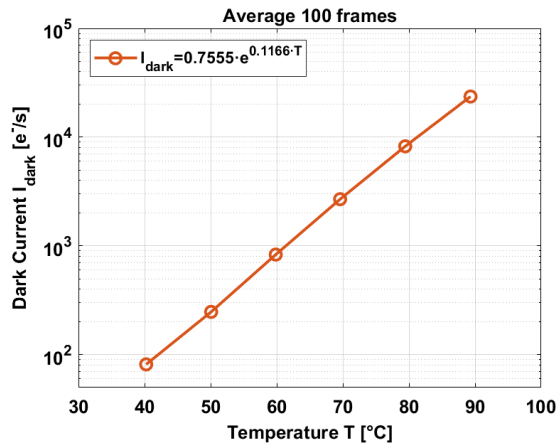


Figure 4: Dark current at high temperatures.

The average dark current at high temperatures is fit by an exponential curve providing the relation between I_{dark} and T .

On the other hand, the nSFTSs exhibit good linearity and accuracy in the temperature range of $-40\text{ }^{\circ}\text{C}$ and $90\text{ }^{\circ}\text{C}$. The average output voltage ΔV_{GS} has a curvature of 0.15% with an average temperature coefficient (TC) of $1.15\text{ mV}/^{\circ}\text{C}$, as shown in Figure 5.

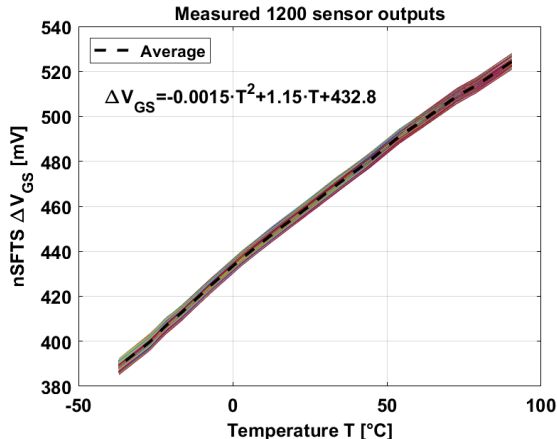


Figure 5: ΔV_{GS} over a temperature range of $-40\text{ }^{\circ}\text{C}$ and $90\text{ }^{\circ}\text{C}$.

After systematic non-linearity removal (by applying a 1st order polynomial), the 3σ inaccuracy was calculated by applying a 2nd order polynomial and it is $\pm 0.55\text{ }^{\circ}\text{C}$, as shown in Figure 6.

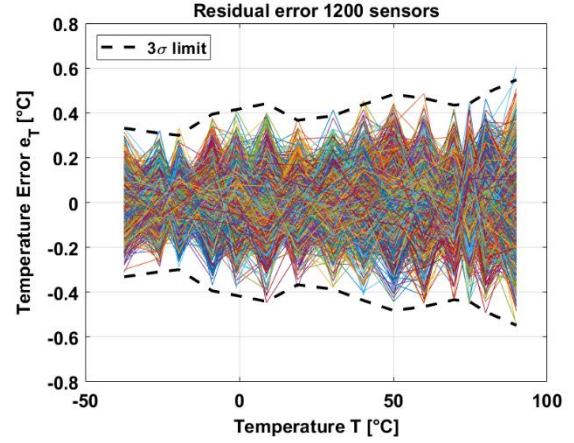


Figure 6: 3σ inaccuracy after systematic removal. $3\sigma = \pm 0.55\text{ }^{\circ}\text{C}$.

An artificial dark reference frame can be generated from the temperature information of each nSFTS and the average dark current, as it was stated in Section II. In this case, an artificial dark reference frame is calculated at $50\text{ }^{\circ}\text{C}$ and at 1 s exposure time. The artificial dark frame is compared to a pre-recorded dark reference frame obtained by using an external closed mechanical shutter on the test CIS device. Figure 7 shows the comparison between frames with closed mechanical shutter and the artificially generated. For simplicity, a smaller piece of the pixel array has been considered.

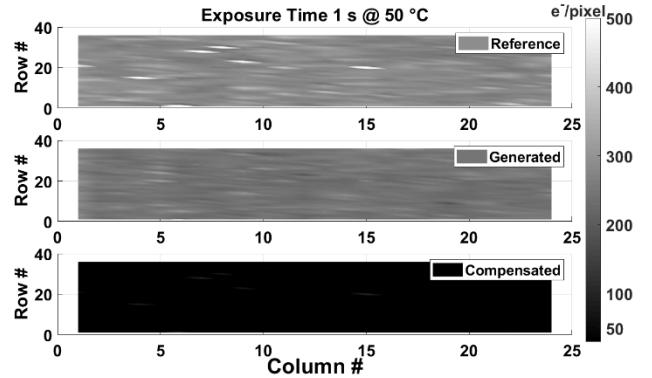


Figure 7: (Top) pre-recorded dark reference frame; (Middle) artificial dark frame ($\Delta V_{GS} \rightarrow T \rightarrow I_{dark} \rightarrow S_{dark}$); (Bottom) subtraction between the dark reference frame (top) and the generated dark frame (middle).

After subtracting the pre-recorded dark reference frame and the artificial dark frame, the dark signal level is reduced from $\sim 300\text{ e}^-/\text{pixel}$ to $\sim 50\text{ e}^-/\text{pixel}$, and the non-uniformity is reduced from 40 e^- to 15 e^- . The compensation is done off-chip. The reduction of the median value and the non-uniformity can be clearly observed when the pre-recorded dark reference frame is compensated at histogram level. The artificial dark frame compensates the pre-recorded frame in its median value (μ) by 82%

and it compensates in its non-uniformity (σ) by 63 %, as shown in Figure 8.

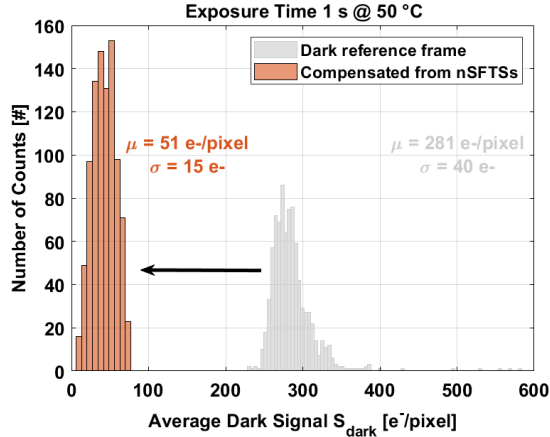


Figure 8: Compensation of the pre-recorded dark reference frame with close mechanical shutter.

The main characteristics of the CIS and the nSFTS are shown in Table 1.

Table 1: Summary of the CIS and nSFTS performance.

CIS		nSFTS	
Characteristic	Value	Characteristic	Value
Type	4T	Type	nMOS
Process [μm]	0.18	Process [μm]	0.18
Array	60×70	Range [$^{\circ}\text{C}$]	-40 to 90
Pixel Area [μm^2]	11×11	Area [μm^2]	11×11
CG [$\mu\text{V}/\text{e}^-$]	78	Resolution [$^{\circ}\text{C}$]	0.1
I_{dark} @ 30°C [e^-/pixel]	50	3σ inaccuracy [$^{\circ}\text{C}$]	± 0.55
		Power [μW]	120

IV. CONCLUSION

A novel technique for dark current compensation of a CIS has been presented. The compensation can be performed in a CIS without the need of a mechanical shutter and the demand for constant temperature of the device. This technique makes used of accurate in-pixel temperature sensors that assist in creating an artificial dark reference frame at a certain exposure time by using the temperature information of the IPTSs and the dark current level of the CIS. The IPTS consists of the nMOS source follower of the pixel itself. When the nSFTS is biased

by sequential ratiometric currents, then the ΔV_{GS} is PTAT. The artificial dark frame has been compared to a pre-recorded dark reference frame with closed mechanical shutter, proving to be highly efficient when compensation is performed. At 50°C and at 1 s exposure time, the artificial dark frame compensates by 82 % in its median value and by 63 % in the non-uniformity.

ACKNOWLEDGMENT

The authors acknowledge TowerJazz for their support in fabricating the prototypes CIS devices.

REFERENCES

- [1] J. Janesick and G. Putman, "Developments and applications of high-performance CCD and CMOS imaging arrays," *Annual Review of Nuclear and Particle Science*, vol. 53, no. 1, pp. 263-300, 2003.
- [2] L.G. McIlrath, "A low-power low-noise ultrawide-dynamic-range CMOS imager with pixel-parallel A/D conversion," *IEEE Journal of Solid-State Circuits*, vol. 36, no. 5, pp. 846-853, 2001.
- [3] C. Hsiu-Yu and K. Ya-Chin, "An ultra-low dark current CMOS imager sensor cell using n+ ring reset," *IEEE Electron Device Letters*, vol. 23, no. 9, pp. 538-540, 2002.
- [4] H.I. Kwon, I.M. Kang, B.G. Park, J.D. Lee and S.S. Park, "The analysis of dark signals in the CMOS APS imagers from the characterization of test structures," *IEEE Transactions on Electron Devices*, vol. 51, no. 2, pp. 178-184, 2004.
- [5] J. Nakamura, "Image Sensors and Signal Processing for Digital Still Cameras," Taylor & Francis Group, pp. 67-72.
- [6] S. Yu-Chuan and W. Chung-Yu, "A new CMOS pixel structure for low-dark-current and large-array-size still imager applications," *IEEE Transactions on Circuits and Systems I: Regular Papers*, vol. 51, no. 11, pp. 2204-2214, 2004.
- [7] X. Wang, "Noise in sub-micron CMOS image sensors," Ph.D. Dissertation, Delft University of Technology, pp. 46-68, 2008.
- [8] P.S. Baranov, V. T. Litvin, D. A. Belous, and A. A. Mantsvetov, "Dark current of the solid-state imagers at high temperature," *IEEE Conference of Russian Young Researchers in Electrical and Electronic Engineering (EIConRus)*, 2017: IEEE, pp. 635-638.
- [9] R. Widenhorn, M. Blouke, A. Weber, A. Rest, and E. Bodegom, "Temperature dependence of dark current in a CCD," *Electronic Imaging*, 2002, vol. 4669, pp. 193-201.
- [10] P. M. Beaudoin, Y. Audet, and V. H. Ponce-Ponce, "Dark current compensation in CMOS image sensors using a differential pixel architecture," *2009 Joint IEEE North-East Workshop on Circuits and Systems and TAISA Conference*, 2009, pp. 1-4.
- [11] R. Widenhorn, A. Rest, M. Blouke, R. Berry, and E. Bodegom, "Computation of dark frames in digital imagers," *Electronic Imaging 2007*, 2007, vol. 6501, pp. 650103-650111.
- [12] A. Abarca, S. Xie, J. Markenhof, and A. Theuwissen, "Integration of 555 temperature sensors into a 64×192 CMOS image sensor," *Sensors and Actuators A: Physical* 2018, vol. 282, pp. 243-250.
- [13] S. Xie, A. Abarca, and A. Theuwissen, "A CMOS-imager-pixel-based temperature sensor for dark current compensation," *IEEE TCAS II: Express briefs* 2020, vol. 67, no. 2, pp. 255-259.
- [14] A. Abarca, and A. Theuwissen, "In-pixel temperature sensors with an accuracy of $\pm 0.25^{\circ}\text{C}$, a 3σ variation of $\pm 0.7^{\circ}\text{C}$ in the spatial noise and a 3σ variation of $\pm 1^{\circ}\text{C}$ in the temporal domain," *Micromachines* 2020, vol. 11, no. 7, 665.